

A New Lorenz System Parameter Determination Method and Applications

A. Orue^a, G. Alvarez^{a,*}, G. Pastor^a, M. Romera^a,
F. Montoya^a and Shujun Li^b

^a*Instituto de Física Aplicada, Consejo Superior de Investigaciones Científicas,
Serrano 144, 28006-Madrid, Spain*

^b*Department of Electronic and Information Engineering, The Hong Kong
Polytechnic University, Hung Hom, Kowloon, Hong Kong SAR, China*

Abstract

This paper describes how to determine the parameter values of the chaotic Lorenz system from one of its variables waveform. The geometrical properties of the system are used firstly to reduce the parameter search space. Then, a synchronization-based approach, with the help of the same geometrical properties as coincidence criteria, is implemented to determine the parameter values with the wanted accuracy. The method is not affected by a moderate amount of noise in the waveform. As way of example of its effectiveness, the method is applied to figure out directly from the ciphertext the secret keys of two-channel chaotic cryptosystems using the variable z as a synchronization signal, based on the ultimate state projective chaos synchronization.

1 Introduction

The feasibility of enslaving two chaotic systems [1] opened the possibility of using the signals generated by chaotic systems as carriers for analog and digital communications and soon aroused great interest as a potential means for secure communications [2]. It is assumed in the literature that chaotic modulation is an adequate means for secure transmission, because chaotic maps present some properties, such as sensitive dependence on parameters and initial conditions, ergodicity, mixing, and dense periodic points, that make them similar to pseudo random noise [3], which has been used traditionally as a masking signal for cryptographic purposes.

* Corresponding author: Email: gonzalo@iec.csic.es

For over a decade a number of secure communication systems have been proposed in which the plaintext message signal $m(t)$ was concealed into the chaotic signal by simply adding it to a system variable $u(t)$ of the sender chaotic generator [4,5,6]; the receiver had to synchronize with the sender to regenerate the chaotic signal $\tilde{u}(t)$ and thus recover the message $m(t)$. This uncomplicated scheme is usually broken by setting apart $u(t)$ and $m(t)$ signals using elemental high pass filtering [7,8,9], or by directly estimating the chaotic signal $u(t)$ via Short's NLD method [10,11].

To avoid this weakness a more elaborated mixing procedure was employed in some recently proposed chaotic cryptosystems: a two-channel transmission technique was used, where an unmodified chaotic system variable was transmitted using the first channel, while a second channel conveyed a signal that was a complicated non-linear combination of the plaintext and another system variable, from which it was impossible to retrieve both separately. The first channel served as synchronizing signal for the chaotic system receiver, then the remaining chaotic system variables were generated and employed at the receiver end to retrieve the plaintext from the second channel signal, using the same system parameters values at sender and receiver [12,13,14].

In the vast majority of chaotic cryptosystems the security relies on the secrecy of the system parameters, which play the role of secret key, hence the determination of the system parameters from the chaotic ciphertext is equivalent to breaking the system.

The contribution of this work is double. First, a novel determination method of the unknown parameters of a Lorenz system, when the waveform of one of its variables is known, is presented in Sec. 2. Then, in Secs. 3 and 4, it is shown how this method can be applied to break some two-channel cryptosystems that use the Lorenz chaotic system. Finally, Sec. 6 concludes the paper.

2 Parameter determination of the Lorenz system

Since 1963 the Lorenz system [15] has been a paradigm for chaos. Consequently, it has been predominantly used in the design of chaotic cryptosystems. It is defined by the following equations:

$$\begin{aligned} \dot{x} &= \sigma(y - x), \\ \dot{y} &= rx - y - xz, \\ \dot{z} &= xy - bz. \end{aligned} \tag{1}$$

where σ , r and b are fixed parameters.

The proposed approach to the problem of Lorenz system parameter determination is based on a homogeneous driving synchronization mechanism [16] between a drive Lorenz system and a response subsystem that is a partial duplicate of the drive system reduced to only two variables, driven by the third variable.

Projective synchronization (PS) is an interesting phenomena firstly described by Mainieri and Rehacek [17]. It consists of the synchronization of two partially linear coupled chaotic systems, sender and receiver, in which the amplitude of the slave system is a scalar multiple, called scaling factor, of that of the sender system in the phase space. The original study was restricted to three-dimensional partially linear systems. Xu and Li [18] showed that PS could be extended to general classes of chaotic systems without partial linearity, by means of the feedback control of the slave system.

The response system is defined by the following equations, in which variable $z(t)$ is used as driving signal:

$$\begin{aligned}\dot{x}_r &= \sigma^*(y_r - x_r), \\ \dot{y}_r &= r^*x_r - y_r - x_rz,\end{aligned}\tag{2}$$

where σ^* and r^* are fixed parameters and the drive variable is z .

As was shown in [16, §III] this drive-response configuration has two conditional Lyapunov exponents, the first one is fairly negative while the second one is of small positive value, thus leading to a slightly unstable system. The consequence is that if the parameters of drive and response systems are identical, then the drive and response variables will become identical (for complete synchronization) or differ only in an scaling factor (for projective synchronization), that depends on the initial conditions of the drive and response systems. However, if the parameters are not exactly equal, then the drive and response variables will be completely different.

When the drive and response systems parameters are equal, the variable $x_r(t)$ will be easily recognizable as the familiar waveform of a Lorenz system, by a supposed human skilled observer. But if drive and response systems parameters are different, the waveforms generated by the response system will be a nonsense mesh some seconds after the beginning of driving, due to the sensitive dependence of chaotic systems on parameter values. This phenomenon could be interpreted by the observer as the consequence of a wrong parameter guessing.

This work describes a criterion, based on the study of some geometric properties of the Lorenz system variables waveforms, to automatically decide if the response system parameters coincide with the drive system parameters or not, by means of the analysis of the $x_r(t)$ waveform of the response system.

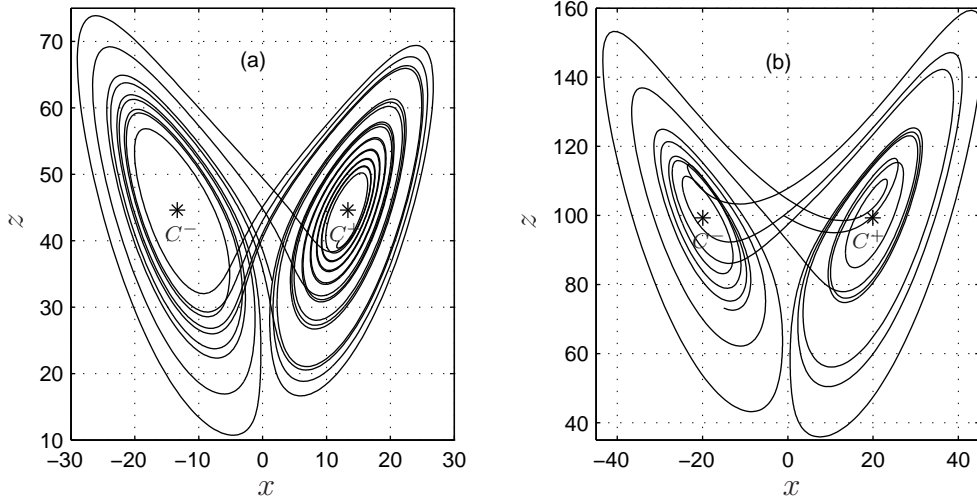


Fig. 1. Lorenz chaotic attractor: (a) parameters $r = 45.6$, $\sigma = 16$ and $b = 4$; (b) parameters $r = 100.3$, $\sigma = 16$ and $b = 4$, showing irregular cycles that not surround the fixed points. The position of the fixed points C^+ and C^- is indicated by asterisks.

This method of recovering the unknown system parameters is applicable in the case of cryptosystems that use the variable $z(t)$ as the driving signal like [13,14]. But it is not applicable to other two-channel cryptosystems driven by $x(t)$ or $y(t)$, like [12], because in those cases both Lyapunov exponents are negative and the drive-response configuration is stable, in despite of being the drive and response parameters moderately different. In those cryptosystems another efficient method of revealing the Lorenz system parameters described by Stojanovski *et al.* is applicable [20].

To minimize the computer workload as much as possible, the parameter search space is previously reduced to a narrow range by means of a simple measure upon the $z(t)$ waveform. Then, all the unknown parameter values are determined with the desired accuracy.

2.1 Lorenz attractor's geometrical properties

According to [15] the Lorenz system has three fixed points. For $0 < r < 1$ the origin of coordinates is a globally stable fixed point; for $1 \leq r < r_c$ the origin becomes unstable giving rise to two other stable twin points C^+ and C^- , of coordinates $C^\pm = (\pm\sqrt{b(r-1)}, \pm\sqrt{b(r-1)}, (r-1))$, being r_c a critical value defined as:

$$r_c = \frac{\sigma(\sigma + b + 3)}{\sigma - b - 1}. \quad (3)$$

When r exceeds the critical value r_c , the system becomes unstable, and its behavior is chaotic.

The Fig. 1(a) shows the well known double scroll Lorenz attractor formed by the projection on the $x - z$ plane, in the phase space, of a trajectory portion extending along 10 sec, where the parameters are $r = 45.6$, $\sigma = 16$ and $b = 4$, the initial conditions are $x_0 = 13.3566$, $y_0 = 13$ and $z_0 = 44.6$, the fixed points C^+ and C^- are indicated by asterisks.

It is a well known fact that the Lorenz attractor trajectory follows two loops, in the vicinity of the fixed points C^+ and C^- , with a spiral-like shape of steadily growing amplitude, jumping from one to the other, at irregular intervals, in a random-like manner though actually deterministic [15]. The trajectory always jumps from a cycle of relative high amplitude to another on the opposite loop generally of smaller amplitude. The spiraling trajectory may pass arbitrarily near to the fixed points, but never reach them while in chaotic regime.

Definition 1. The portions of the attractor trajectory that consist of a revolution of 360° beginning after a change of sign of x and y are *irregular cycles*. The portions of the trajectory that constitute a complete spiral revolution of 360° and do not begin after a change of sign of x and y are *regular cycles*.

Remark 1. Regular cycles always surround the fixed points C^+ or C^- , taking them as centers of a growing spiral.

Remark 2. Irregular cycles usually surround the fixed points C^+ or C^- ; but sometimes may not surround them, instead the trajectory may pass slightly above them in the $x - z$ plane. This phenomenon is illustrated in the Fig. 1(b), with system parameters $r = 100.3$, $\sigma = 16$ and $b = 4$ and initial conditions $x_0 = -1$, $y_0 = 35.24$ and $z_0 = 100$.

Definition 2. The *attractor eyes* are constituted by the two neighborhood regions around the fixed points that are not filled with regular cycles. The eye centres are the fixed points C^+ or C^- .

Definition 3. The *eye aperture* x_a and z_a of the variables x and z , for a particular time period, is the smallest distance between the maxima and minima of $|x(t)|$ and $z(t)$, respectively, of the regular cycles, measured along this time period.

Figure 2 illustrates the first 2.25 s of another version of the Lorenz attractor of Fig. 1(b), folded around the z axis and formed by the projection on the $x - z$ plane, in the phase space, of a trajectory portion of $z(t)$ and $|x(t)|$. The trajectory portion drawn with solid thick line is the regular cycle closest to the fixed points C^\pm , from which the eye aperture of x_a and z_a can be determined. The trajectory portion drawn with dashed thick line belongs to the preceding irregular cycle.

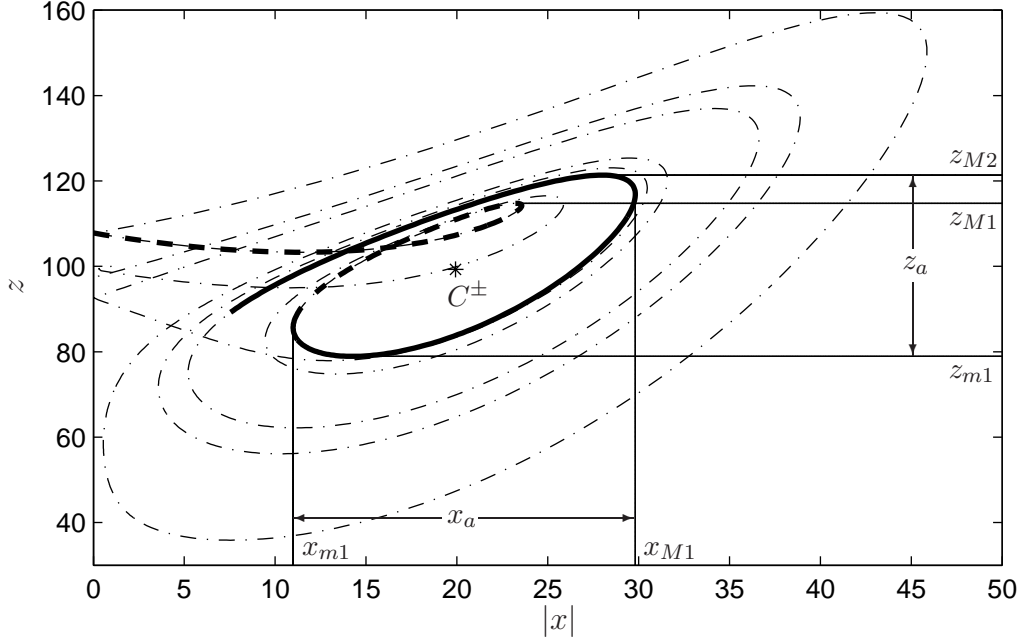


Fig. 2. First 2.25 s of a version of the Lorenz attractor of Fig. 1(b), folded around the z axis. The solid thick line trajectory portion is the regular cycle closest to the fixed points C^\pm . The dashed thick line trajectory portion is the preceding irregular cycle.

2.2 Reduction of the parameters search space

The geometrical properties of Lorenz system allows for a previous reduction of the search space of the r parameter, before carrying out the accurate parameter determination, taking advantage of the relation of the system parameter r with the coordinates $z_{C^+} = z_{C^-} = r - 1$ of the fixed points C^+ and C^- and Eq. (3). The estimated value $z_{C^\pm}^*$ of the fixed points coordinates $z_{C^+} = z_{C^-}$ was calculated from the variable $z(t)$ using following algorithm:

- (1) compile a list of all the relative maxima and minima of $z(t)$,
- (2) exclude all the minima belonging to an irregular cycle from the list,
- (3) retain the biggest relative minimum z_{m1} , among the remaining list elements,
- (4) select the two maxima z_{M1} , z_{M2} immediately preceding and following z_{m1} , respectively,
- (5) calculate the spiral centre as $z_{C^\pm}^* = (\frac{1}{3}z_{M1} + \frac{2}{3}z_{M2} + z_{m1})/2$.

There is no need to find a rule of growing for the spiral radius, since the optimal values of the two weights of z_{M1} and z_{M2} , in the preceding $z_{C^\pm}^*$ formula, can be determined experimentally.

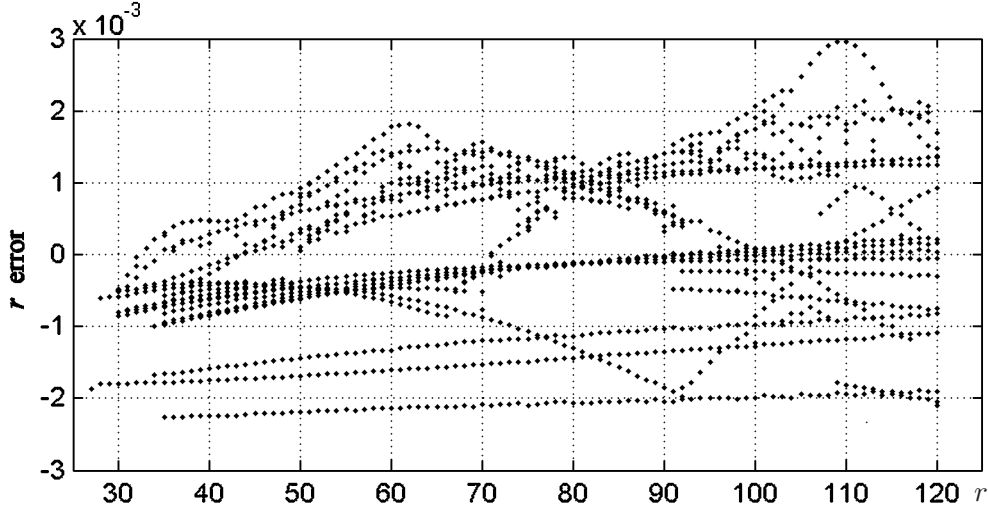


Fig. 3. Parameter r estimation error, when calculated from the fixed point coordinate $z_{C\pm}^*$, for different combinations of system parameters σ and b .

The minima of the irregular cycles were discarded because they are inappropriate for the fixed point's z coordinate calculation, due to the fact that irregular cycles may not take the fixed points as centres. Those cycles are very easy to detect from the $z(t)$ waveform: they are the first minima that comes after a previous minimum of smaller value.

Figure 3 illustrates the relative error when the value of r is estimated as $r^* = z_{C\pm}^* + 1$, for values of r^* ranging from the critical value $r^* = r_c$ to $r^* = 120$, in increments of $\Delta r^* = 1$, for 15 different combinations of system parameters, $\sigma = (6, 10, 13, 16, 20)$ and $b = (2, 8/3, 4)$; the analyzed time was 200 s of the $z(t)$ waveform. As can be seen, the maximum relative error spans from -0.23% to $+0.3\%$. In this way, when trying to guess the value of r from the waveform of $z(t)$, the effective search space may be reduced to a narrow margin of less than 0.6% of the computed value $r^* = z_{C\pm}^* + 1$.

The presence of moderate noise added to the $z(t)$ waveform did not affect the precision of the measure. Some tests were carried adding either white gaussian noise or sinusoidal signals, of a level 30 db below $z(t)$. The resultant relative error in the guess of r^* was still inferior to $\pm 0.2\%$, for $\sigma = 16$ and $b = 4$. But for not so moderated values of added noise the increase of relative error was noticeable; i.e. when the noise reached a value of 20 db below $z(t)$ the relative error raised to about $\pm 1\%$.

The search space of σ^* can also be delimited. Assuming that $r > r_c$, $b \geq 0$ and $\sigma > 0$, it follows from Eq. (3) that:

$$0 > \sigma^2 + (b + 3 - r)\sigma + r(b + 1) > \sigma^2 + (3 - r)\sigma, \quad (4)$$

that yields a very conservative margin of $0 < \sigma < r - 3$.

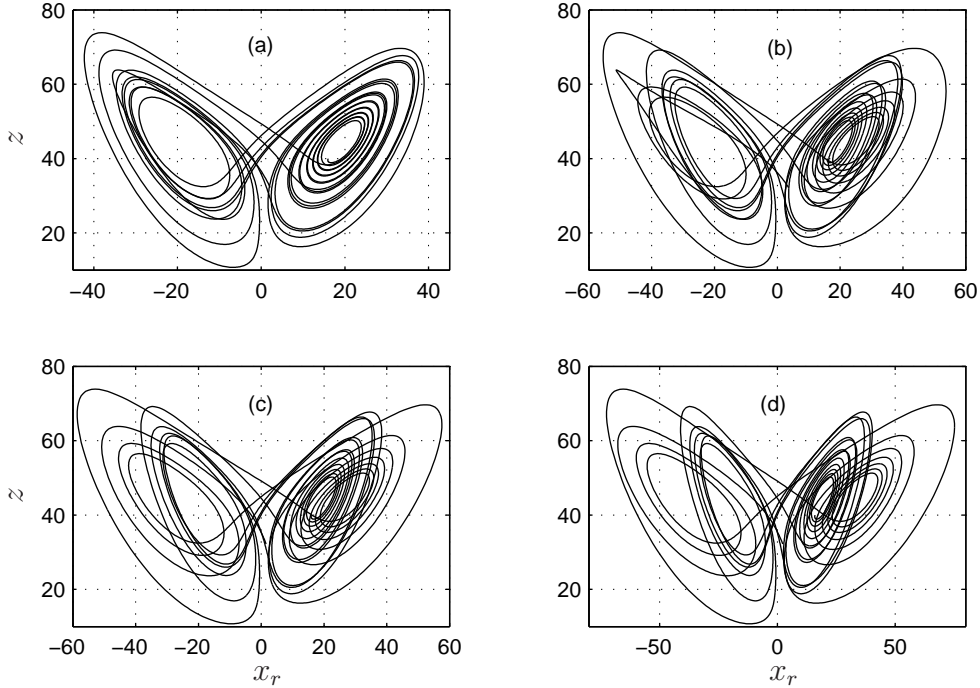


Fig. 4. Lorenz attractor formed by the projection on the $x_r - z$ plane, in all cases the drive parameter are the same: $\sigma = 16$ and $r = 45.6$; but response parameter values are different: (a) $\sigma^* = \sigma$, $r^* = r$; (b) $\sigma^* = \sigma$, $r^* = 45.61$; (c) $\sigma^* = 15.65$, $r^* = r$; (d) $\sigma^* = 15.65$, $r^* = 45.61$.

2.3 Accurate parameter determination

Once the search space of the parameters is fixed, a homogeneous driving synchronization based procedure can be implemented to determine the approximate values r^* and σ^* with any desired accuracy. For this purpose, the response system described by Eq. (2) was used.

When the synchronizing signal is fed to the response and the parameters of both systems agree, i.e. $r^* = r$ and $\sigma^* = \sigma$, the variables x_r and y_r follow the drive signals x and y with a scale factor that depends on the initial conditions. If the parameters of both systems do not agree, i.e. $r^* \neq r$ and/or $\sigma^* \neq \sigma$, the variables waveforms of drive and response systems will differ absolutely, even if the initial conditions are the same. After a few system iterations, all waveforms generated with different parameters values are nearly alike, but as the number of iterations grow, the waveforms generated with different parameter values begin to diverge, due to the conditional positive Lyapunov exponent of the drive-response configuration. For large number of iterations, even the smallest difference in parameters values leads to a serious disagreement of drive and response waveforms.

Figure 4 shows the double scroll Lorenz attractor formed by the projection

on the $x_r - z$ plane when four possible cases of parameter coincidence are considered. In Fig. 4(a) both parameters of drive and response systems are equal. It can be seen that the attractor is similar to the illustrated in Fig. 1(a), being the difference the disagreement in the horizontal scale due to different initial conditions, it can be also observed that the attractor eye is quite open. In Fig. 4(b) one parameter coincides, but the other differs: $\sigma = \sigma^* = 16$, $r = 45.6$ and $r^* = 45.61$, it can be seen that eye aperture has diminished considerably with respect to the former case. In Fig. 4(c) the coinciding parameter is $r = r^* = 45.6$, the differing one is $\sigma = 16$ and $\sigma^* = 15.65$, it can be seen that the eye aperture has diminished even more. Finally, in Fig. 4(d) both parameters differ $r = 45.6$, $r^* = 45.61$, $\sigma = 16$ and $\sigma^* = 15.65$, it can be seen that the eye is completely closed, i.e. the eye x -aperture x_a is negative. Similar measures were carried out for a great variety of drive parameter values with identical results. When the differences between the true parameter values and the guessed values $r - r^*$ and $\sigma - \sigma^*$ are big, the eye aperture closes after very few cycles, but for progressively diminishing differences between parameters the number of cycles needed to obtain a closing eye are increasing.

The value of the eye x -aperture x_a of the variable $x_r(t)$ was computed for many sets of parameters values. It was found in all cases that its maximum value was reached when $r^* = r$ and $\sigma^* = \sigma$. For these parameter values the variables x and x_r are completely synchronous but differ only in a proportionality factor. Hence the maximum eye aperture is an excellent numerical criterium for evaluating the synchronism between drive and response systems.

The eye x -aperture x_a of the variable $x_r(t)$, was calculated with the following algorithm:

- (1) compile a list of all relative maxima and minima of $\text{abs}(x_r(t))$,
- (2) exclude all the maxima belonging to an irregular cycle from the list,
- (3) retain the smallest relative maximum x_{M1} , among the remaining maxima,
- (4) select the biggest minimum x_{m1} , among all the minima,
- (5) calculate the eye aperture as $x_a = x_{M1} - x_{m1}$.

3 Application to cryptanalysis of a multiplexed two-channel projective synchronization cryptosystem

After their research in PS, Xu and Li proposed a secure communication scheme based on PS chaotic masking [14], that was shown to be breakable by filtering and by generalized synchronization using the feedback of the plaintext recovery error [19].

In a recent article Wang and Bu [13] proposed a new encryption scheme also

based on PS. Following [17], the state vector of a partially linear system of ordinary differential equations was broken in two parts (\mathbf{u}, z) . The equation for $z(t)$ was nonlinearly related to the other variables, while the equation for the rate of change of the vector \mathbf{u} was linearly related to \mathbf{u} through a matrix M that may depend on the variable $z(t)$. It was employed a sender system (\mathbf{u}_s, z) , a receiver system (\mathbf{u}_r, z) , and an auxiliary system (\mathbf{u}_c, z) defined as:

$$\begin{aligned}\dot{\mathbf{u}}_s &= M(z) \cdot \mathbf{u}_s, & \dot{z} &= f(\mathbf{u}_s, z), \\ \dot{\mathbf{u}}_r &= M(z) \cdot \mathbf{u}_r, \\ \dot{\mathbf{u}}_c &= M(z) \cdot \mathbf{u}_c,\end{aligned}\tag{5}$$

where $\mathbf{u}_s = (x_s, y_s)$, $\mathbf{u}_r = (x_r, y_r)$, and $\mathbf{u}_c = (x_c, y_c)$. When PS takes place $\lim_{t \rightarrow \infty} \|\mathbf{u}_s - \alpha \mathbf{u}_r\| = 0$, being α a constant depending on the initial conditions of $\mathbf{u}_r(0)$ and $\mathbf{u}_s(0)$.

The ciphertext $s(t)$ was defined as a composition in function of time of the shared scalar variable $z(t)$ and the scalar variable $x_s(t)$, described as:

$$s(t) = \begin{cases} x_s(t), & n\Delta t \leq t \leq n\Delta t + \delta t, \\ z(t), & n\Delta t + \delta t < t \leq (n+1)\Delta t, \end{cases}\tag{6}$$

being $n = (0, 1, 2, \dots)$, while Δt and δt are two time intervals so that $\delta t \ll \Delta t$.

The ciphertext plays the double roles of the driving signal for chaos synchronization between the sender and receiver, by means of $z(t)$, and the message carrier through $x_s(t)$.

It is supposed that the plaintext message $i(t)$ was previously discretized in time, in the form of a string of bits or a string of samples, i_n . In the first case, the bits are coded as $+1$ or -1 . In the second case, the analog signal is sampled at a rate of $1/\varepsilon$ samples per second, where ε is the sampling period.

The encryption of a plaintext $i(t)$ was achieved as follows: at the beginning of each time interval Δt , during a much shorter time interval δt , the sender system vector \mathbf{u} is forcibly modified in the following way:

$$\mathbf{u}_s(t_n) = i_n \mathbf{u}_c(t_n),\tag{7}$$

and at the end of the time interval δt the entire system was let freely evolving until the beginning of the next time period Δt .

Figure 5 illustrates the waveform of the ciphertext. It can be seen that $s(t)$ is a discontinuous signal that agrees most of the time with the function $z(t)$, but jumps to the value of $x_s(t)$ during a small time interval δt every Δt seconds.

The function $z(t)$ was easily recovered, at the receiver end, by filtering out

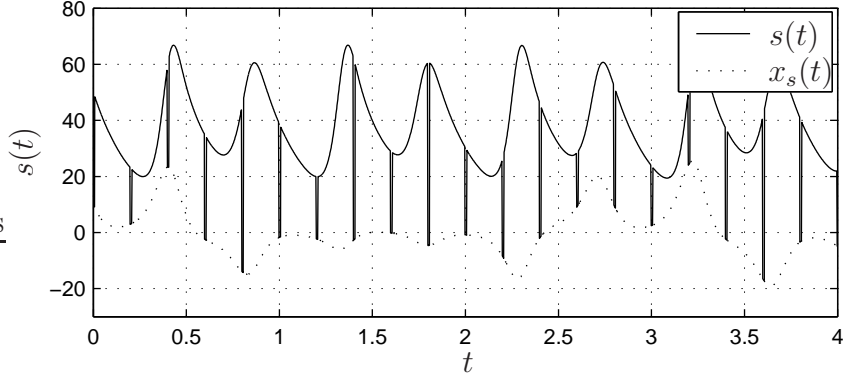


Fig. 5. Ciphertext $s(t)$, for $\Delta t = 0.2$ and $\delta t = 0.01$ (solid line) and scalar variable $x_s(t)$ (dotted line).

the spikes. The final signal distortion is negligible due to the short spike time length δt related to their repetition period Δt .

To recover the plaintext, instead of using the signal $x_s(t)$, which is not available at the receiver end, the average value of the spikes $\bar{x}_s(t)$ for $n\Delta t \leq t \leq n\Delta t + \delta t$ was employed. Thanks again to the fact that $\delta t \ll \Delta t$, it can be considered that $\bar{x}_s(t)$ is a good approximation of $x_s(t)$.

The recovered plaintext $i'_n(t)$ at the receiver end was calculated as:

$$i'_n(t) = \frac{\bar{x}_s(t_n)}{x_r(t_n)} = \frac{\bar{y}_s(t_n)}{y_r(t_n)} \quad (8)$$

If the initial conditions of the auxiliary system and the receiver system are identical, the original plaintext and the retrieved plaintext will agree: $i'_n(t) = i_n(t)$. However, if the initial conditions are different, the retrieved plaintext will be not equal, but proportional, to the original plaintext: $i'_n(t) = c i_n(t)$. Due to PS between the sender and receiver, here c is a constant.

For practical purposes, the present system is a two-channel communication system, with the particularity that both channels, one continuous and another sampled, are transmitted in a multiplexed way and separated at the receiving end.

In [13, §3] an example was presented using similar sender-receiver circuits to the ones described in [21], based on the Lorenz system, see Eq. (1), with parameter values:

$$\sigma = 16.0, \quad r = 45.6, \quad b = 4.0, \quad \Delta t = 0.2, \quad \delta t = 0.01, \quad \varepsilon = 0.001. \quad (9)$$

It was shown that an absolute error of $\Delta r^* = 0.001$ in the value of the receiver parameter r^* leads to a plaintext recovery failure, and it was asserted that a similar deviation in the receiver parameter σ^* value has the same effect.

Hence, although not clearly stated by the authors of [13], it can be estimated that in this cryptosystem the parameter values play the role of secret key. In every cryptosystem, the key should be completely specified [22].

The authors of [13] claimed that this method has some remarkable advantages over other chaos-based secure communication schemes, because it is not possible to extract the plaintext directly from the ciphertext by means of an error function attack, due to the system high sensitivity to the parameter values. Moreover, conventional return map attacks exploiting the perturbation of the sender dynamics are also avoided, because the modulation procedure only affects the initial values of the trajectories in the phase space.

3.1 System parameters recovery procedure

In the system proposed in [13], the variable $z(t)$ was extracted at the receiver end from the ciphertext $s(t)$ and used to achieve the receiver synchronization. This fact allows mounting an attack against the system parameters, whose values can be accurately determined.

In our simulation, the same sender used in [13] was employed as a drive system, described by Eq. (1). As the intruder's receiver the response system described by Eq. (2) was used. The same sender parameters of the authors' example were used. The initial conditions of the sender were arbitrarily chosen as $x_s(0) = 40$, $y_s(0) = 40$, $z(0) = 40$, because in [13] there was no details about them. The initial conditions of the intruder's response system were arbitrarily chosen as $x_r(0) = 70$, $y_r(0) = 7$.

The adequate searching ranges for the parameters r^* and σ^* were determined as follows: applying the algorithm described in the Section 2.2 to 200 s of the $z(t)$ waveform, it was found that the fixed point z coordinate was $z_{C\pm}^* = 44.5943$, that corresponds to $r^* = 45.5943$ (very close to the true value $r = 45.6$); hence a practical search range of r^* going from $r^* = 45.50$ to $r^* = 45.70$ was selected, equivalent to an error allowance ranging from -0.23% to $+0.2\%$, compliant with Fig. 3. The search space of σ^* , according to Eq. (4), should be comprised in the range $0 < \sigma^* < 42.70$.

Figure 6 illustrates the r^* and σ^* determination method using the procedure described in S. 2.3, that is accomplished in five steps. In the first step, the eye aperture of the receiver x_r variable was measured along a period of 25 s, equivalent to 55 periods of $z(t)$. The measure was made for each of the 210 different sets of parameter values obtained varying r^* from $r^* = 45.50$ to $r^* = 45.70$, in increments of $\Delta r^* = 0.05$, and σ^* from $\sigma^* = 1$ to $\sigma^* = 42$, in increments of $\Delta \sigma^* = 1$. The result is illustrated in Fig. 6 (a). It can be seen that for most combinations of parameter values the aperture is negative,

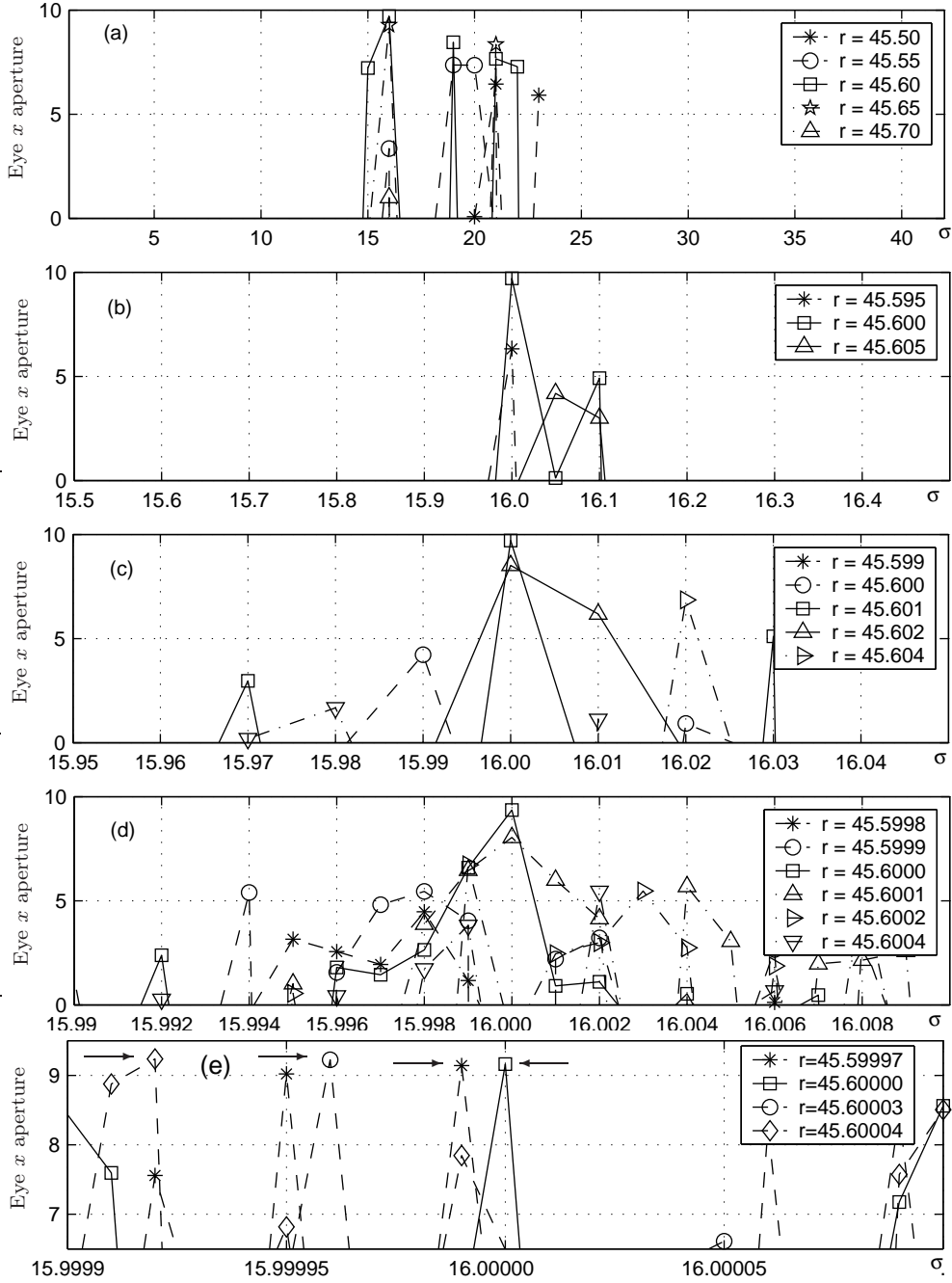


Fig. 6. Intruder receiver eye aperture x_r for various measure periods: (a) 25 s; (b) 80 s; (c) 250 s; (d) 800 s; (e) 800 s

i.e. the corresponding parameter values are far from the right value; the best values for σ^* are comprised between $\sigma^* = 15.5$ and $\sigma^* = 16.5$, while the best values for r^* are comprised between $r^* = 45.55$ and $r^* = 45.65$. Those values are taken as the search limits for the next step. The mesures were done, in the second, third and fourth steps, during periods of 80 s, 250 s and 800 s respectively, the results are depicted in Figs. 6(b), 6(c) and 6(d).

If the available ciphertext was unlimited, the next measure step could be done over a period longer than 800 s until the desired parameter precision could be reached. But let us suppose that there is no more than 800 s of available ciphertext. In that case, the only choice is to constrict the search space around the last best result obtained, with a growing resolution, until a situation is reached in which it becomes impossible to decide which is the best parameter value. The Fig. 6 (e) illustrates this situation, it was obtained keeping the last measure period of 800 s, but narrowing the search space around the last best result obtained. It can be seen that the discrimination limit of the identification method was reached for that period of measure, because multiple peaks gave approximately the same eye aperture of $x_a \approx 9.2$. The four peaks of greater amplitude suggest four sets of equally plausible potential candidates of response system parameter sets, one of them is the right one $r_0^* = r = 45.60000$, $\sigma_0^* = \sigma = 16.00000$, the other three are slightly inexact, they differ in the seventh significative digit from the right value: $r_1^* = 45.59997$, $\sigma_1^* = 15.99999$; $r_2^* = 45.60003$, $\sigma_2^* = 15.99996$ and $r_3^* = 45.60004$, $\sigma_3^* = 15.99992$.

The Figs. 7(a), 7(b) and 7(c) illustrate the 800 first seconds of the waveform of $x_r(t)$ plotted against $x(t)$, for the three inexact system parameter sets. It can be seen that the $x_r(t)$ and $x(t)$ waveforms are perfectly correlated in all the three cases despite of the parameter values little inexactitude. The different initial conditions are the cause of the initial transitory, that lasts only 0.5 s and of the different scale amplitudes of the waveforms. This means that any of the four potential candidates of response system parameter sets may be used indistinctly to generate the $x_r(t)$ waveform without noticeable error, for the limited time period that was considered for their determination.

For practical purposes, a limited precision in the determination of the parameters is not a shortcoming, because the degree of coincidence of the eye apertures x_{a1} and of x_{a2} of two waveforms of $x_{i1}(t)$ and $x_{i2}(t)$, corresponding to two different sets of response system parameters, is a measure of the degree of coincidence between both waveforms. This means that if two sets of slightly different response system parameters have the same eye apertures, computed along a limited time period, the corresponding waveforms are practically equal during this time.

On the contrary, the parameter values of Fig. 7 (d) correspond to the example of [13], with parameter values $r_4^* = 45.601$ and $\sigma_4^* = 15.999$, that undergo a guessing error on the fifth significative digit. Such error was considered in [13] unacceptable for correct plaintext recovery. Effectively, it can be seen in Fig. 7 (d) that $x_r(t)$ and $x(t)$ waveforms are not correlated at all.

If a greater precision in the parameter determination is needed, the period of measure could be accordingly enlarged. The maximum allowable precision is

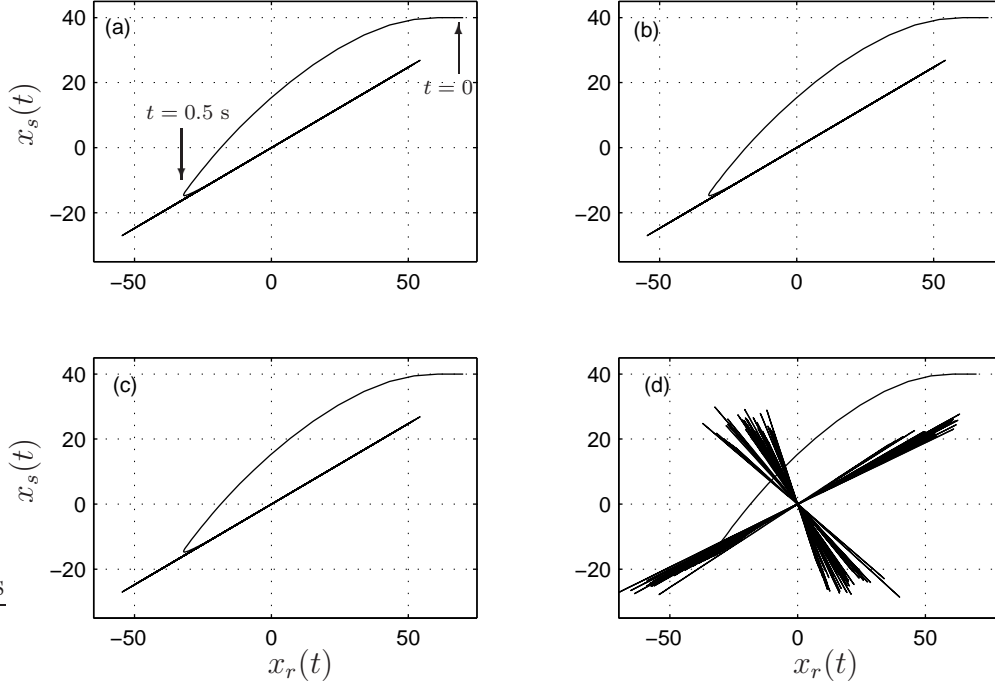


Fig. 7. First 800 s of the intruder receiver phase portrait, for various sets of response system parameters: (a) $r^* = 45.59997$, $\sigma^* = 15.99999$; (b) $r^* = 45.60003$, $\sigma^* = 15.99996$; (c) $r^* = 45.60004$, $\sigma^* = 15.99992$; (d) $r^* = 45.601$, $\sigma^* = 15.999$.

limited by the lifespan of the intercepted communication. To get an infinite precision an infinite measure period time will be needed. The first steps take very small time to compute, because the involved number of samples is short, but the last step is much more time consuming, because the involved number of samples is very large.

When dealing with very long encrypted messages it may be unpractical to expand the parameter computation time to the whole message length, because the computation time may become huge. It is better to divide the message in fractions of not more than the equivalent of 1000 s of the Lorenz system, and repeat the parameter determination procedure for each fraction. In that way it may happen that the found parameters will be different for each message fraction.

Once the best values of r^* and σ^* are determined, the plaintext can be retrieved in the same way as the legal key owner does.

4 Application to cryptanalysis of a two separated channels projective synchronization cryptosystem

In a recent paper Li and Xu [14] proposed a secure communication scheme based on PS chaotic masking. They illustrated the feasibility of the scheme with two examples, one of them was based on the Lorenz system, with sender variables $x_s(t)$, $y_s(t)$ and $z(t)$. The transmitted signals were the Lorenz system shared scalar variable $z(t)$ and the ciphertext signal, defined as $U(t) = x_s(t) + y_s(t) + m(t)$, where $m(t)$ was the plaintext. The retrieved plaintext was calculated by the authorized receiver as $m(t) = U(t) - (x_r(t) + y_r(t))/\alpha$, where α is the PS scaling factor and $x_r(t)$, $y_r(t)$ are the variables generated by the response system. The authors claimed that the lack of knowledge of the value of α by an intruder was an important feature to assure the information security. In their example the system parameter values were $\{\sigma, r, b\} = \{10, 60, 8/3\}$, the scaling factor was $\alpha = 5$ and the plaintext was the sound signal coming from a water flow, of unknown frequency spectrum and about 0.2 units of amplitude, i.e. approximately 0.005 times the amplitude of $x_r(t) + y_r(t)$.

We simulated this cryptosystem with arbitrarily chosen sender initial conditions $x_s(0) = 3$, $y_s(0) = 3$, $z(0) = 20$ because there was no details about them in [14]. The intruder response system initial conditions were chosen equal to corresponding sender initial conditions times the desired scaling factor $\alpha = 5$, that is: $x_r(0) = 15$ and $y_r(0) = 15$. As plaintext message was chosen the function $m(t) = 0.2 \sin(2\pi 30 t)$, i.e. a low frequency tone of similar amplitude to the authors example.

To break this scheme the same determination procedure described in the precedent section was employed. First, using the algorithm of Sec. 2.2, it was found that the fixed point z coordinate was $z_{C^\pm}^* = 58.9766$, that corresponds to $r^* = 59.9766$ (very close to the true value $r = 60$); hence a practical search range of r^* going from $r^* = 59.8$ to $r^* = 60.2$ was selected, equivalent to an error allowance of $\pm 0.33\%$, compliant with Fig. 3 error margins. The search space of σ^* , according to Eq. (4), should be comprised in the range $0 < \sigma^* < 57$.

Figure 8 illustrates the first and fifth steps of the r^* and σ^* determination procedure, that was accomplished with the same method described in the precedent section. In the first step, the eye aperture of the receiver x_r variable was measured along a period of 8 s, varying r^* from $r^* = 59.8$ to $r^* = 60.2$, and σ^* from $\sigma^* = 0$ to $\sigma^* = 57$. The result is illustrated in Fig. 8 (a). As in the previous section it was supposed that the available ciphertext had a length of 800 s. In Fig. 8 (b) it can be seen that the discrimination limit of the identification method was reached for that period of measure, giving multiple peaks approximately the same eye aperture.

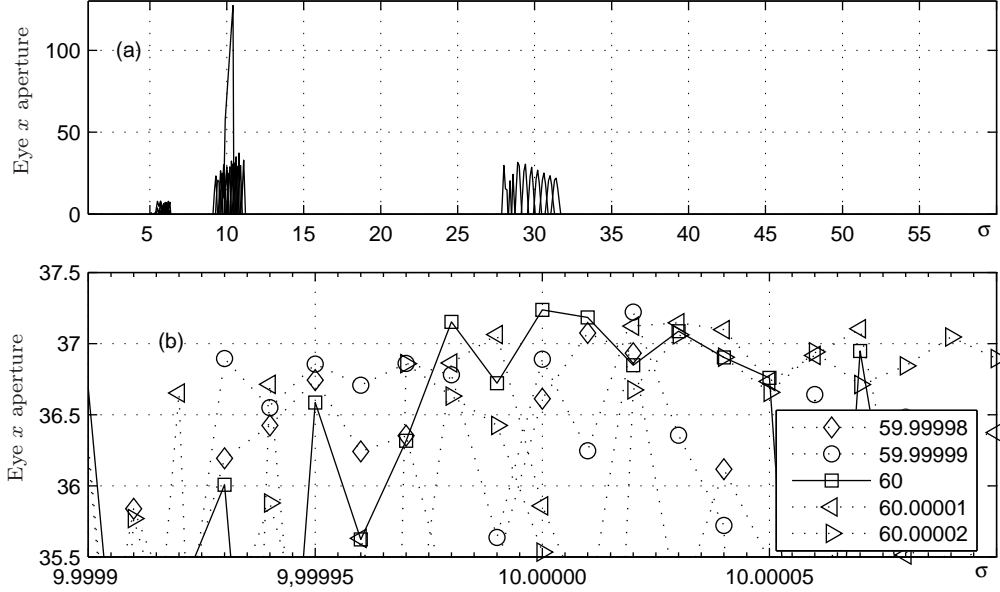


Fig. 8. Intruder receiver eye aperture x_r for various measure periods: (a) 8 s, with $r^* = 59.8$ to $r^* = 60.2$; (b) 800 s, with $r^* = 59.9999$ to $r^* = 60.0001$.

The four peaks of greater amplitude suggest four sets of plausible potential candidates of response system parameter sets. The greatest of them, with an eye aperture $x_{a0} = 37.25$, is the right one: $r_0^* = r = 60$, $\sigma_0^* = \sigma = 10$; the three following candidates, in descending order of eye aperture, are slightly inexact, differing in the seventh significant digit from the right value: $r_1^* = 59.99999$, $\sigma_1^* = 10.00002$ ($x_{a1} = 37.23$); $r_2^* = 60$, $\sigma_2^* = 10.00001$ ($x_{a2} = 37.18$); and $r_3^* = 60$, $\sigma_3^* = 9.99998$ ($x_{a3} = 37.15$).

The determination of the approximated value of the scaling factor α^* may be achieved by dividing, sample by sample, a time period T of the ciphertext by the corresponding period of response system sum of variables and taking the average along that time period:

$$\begin{aligned} \alpha^* &= \overline{\left(\frac{x_s(t) + y_s(t) + m(t)}{x_r(t) + y_r(t)} \right)} \\ &= \overline{\left(\frac{x_s(t) + y_s(t)}{x_r(t) + y_r(t)} \right)} + \overline{\left(\frac{m(t)}{x_r(t) + y_r(t)} \right)} \end{aligned} \quad (10)$$

where $\overline{f(t)}$ denotes the temporal average of $f(t)$ over a period T . In the case that $m(t)$ has zero mean, as in the example given in [14], the last quotient vanishes since $m(t)$ is independent of $x_r(t) + y_r(t)$, while the mean of the first quotient of Eq. 10 reveals the value of α^* . This simple procedure may be slightly inexact due to divide-by-zero problems, so the low amplitude samples were eliminated and the following algorithm was used to determine α^* with more accuracy:

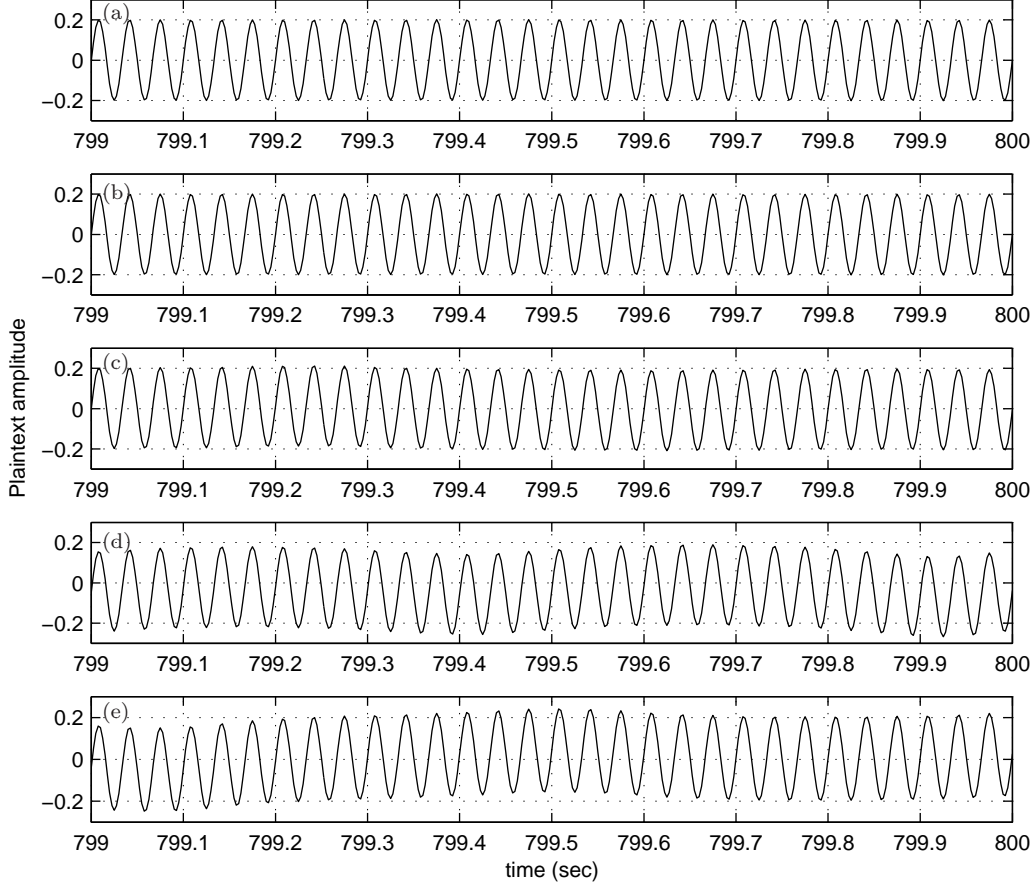


Fig. 9. Last second of plaintext. (a) Original message. Retrieved plaintext for four sets of response system parameters: (b) $r_1^* = 60$, $\sigma_1^* = 10$; (c) $r_1^* = 59.99999$, $\sigma_1^* = 10.00002$; (d) $r_2^* = 60$, $\sigma_2^* = 10.00001$; (e) $r_3^* = 60$, $\sigma_3^* = 9.99998$.

- (1) select a collection of samples of $x_r(t)$ and $y_r(t)$, corresponding to the 800 first seconds of the waveform,
- (2) calculate the maximum value M_{x+y} of the collection of $|x_r(t) + y_r(t)|$ samples,
- (3) compile a list of all the exact sampling times t_{js} for which $|x_r(t_{js}) + y_r(t_{js})| > 0.3 M_{x+y}$ and count the number of them ns ,
- (4) calculate the scaling factor as $\alpha^* = \frac{1}{ns} \sum_1^{ns} \frac{x_r(t_{js}) + y_r(t_{js})}{U(t_{js})}$.

The result was $\alpha^* = 5.000038$, for all the four parameter sets previously identified, which represent a relative error of 7×10^{-6} related to α , that will affect the recovering of $m(t)$ adding a negligible noise of 63 db below its amplitude.

The retrieved plaintext was then calculated as:

$$m^*(t) = U(t) - \frac{x_r(t) + y_r(t)}{\alpha^*} = x_s(t) + y_s(t) + m(t) - \frac{x_r(t) + y_r(t)}{\alpha^*} \quad (11)$$

The Fig. 9 illustrate the plaintext waveform between the seconds 799 and 800 of the the original message $m(t)$ and four recovered messages $m^*(t)$, for the four system parameter sets previously identified. It can be seen that the retrieved waveform corresponding to the first and second set of intruder receiver parameters is completely equal to the original plaintext, while the third and fourth parameters sets cause a small distortion of the retrieved plaintext; note that the distortion increases as the eye aperture goes down, as expected. Nevertheless any of the four potential candidates of response system parameter sets may be used indistinctly to gain access to the encrypted information without significant error, for the limited time period that was considered for their determination.

5 Simulations

All results were based on simulations with MATLAB 7, the Lorenz integration algorithm was a four-fifth order Runge-Kutta with an absolute error tolerance of 10^{-9} , a relative error tolerance of 10^{-6} , and a sampling frequency of 400 Hz.

6 Conclusion

This work describes a novel Lorenz system parameter determination procedure, based on the measure of some attractor geometrical properties, with the help of a homogeneous driving synchronization mechanism. The method is applicable to the cryptanalysis of a two-channel chaotic cryptosystem that uses the variable z as a synchronization signal, allowing for the system secret key recovery and evincing that such systems are not suitable for secure communications. The method is not applicable to break two-channel chaotic cryptosystems that use the variable x or y as a synchronization signal.

Acknowledgements

This work was supported by Ministerio de Ciencia y Tecnología of Spain, research grant SEG2004-02418, and by The Hong Kong Polytechnic University's Postdoctoral Fellowships Scheme under grant no. G-YX63.

References

- [1] L. M. Pecora, T. L. Carroll, Synchronization in chaotic systems, *Phys. Rev. Lett.* 64 (1990) 821–824.
- [2] T. Yang, A survey of chaotic secure communication systems, *Int. J. Comput. Cognit.* 2 (2004) 81–130.
- [3] R. L. Devaney, *A first course in chaotic dynamical systems*, Addison-Wesley, Reading, MA., 1992.
- [4] M. Boutayeb, M. Darouach, H. Rafaralahy, Generalized state-space observers for chaotic synchronization and secure communication, *IEEE Trans. Circuits Syst. I-Fundam. Theor. Appl.* 49 (3) (2002) 345–349.
- [5] Q. Memon, Synchronized chaos for network security, *Comput. Commun.* 26 (2003) 498–505.
- [6] S. Bowong, Stability analysis for the synchronization of chaotic systems with different order: application to secure communication, *Phys. Lett. A* 326 (1-2) (2004) 102–113.
- [7] G. Alvarez, F. Montoya, M. Romera, G. Pastor, Breaking two secure communication systems based on chaotic masking, *IEEE Trans. Circuits Syst. II-Analog Digit. Signal Process.* 51 (10) (2004) 505–506.
- [8] G. Alvarez, S. Li, Breaking network security based on synchronized chaos, *Comput. Commun.* 27 (2004) 1679–1681.
- [9] G. Alvarez, L. Hernández, J. Muñoz, F. Montoya, S. Li, Security analysis of communication system based on the synchronization of different order chaotic systems, *Phys. Lett. A* 345 (4) (2005) 245–250.
- [10] K. M. Short, Steps toward unmasking secure communications, *Int. J. Bifurcation Chaos* 4 (4) (1994) 959–977.
- [11] K. M. Short, Signal extraction from chaotic communications, *Int. J. Bifurcation Chaos* 7 (7) (1997) 1579–1597.
- [12] Z. P. Jiang, A note on chaotic secure communication systems, *IEEE Trans. Circuits Syst. I-Fundam. Theor. Appl.* 49 (1) (2002) 92–96.
- [13] B-H. Wang, S. Bu, Controlling the ultimate state of projective synchronization in chaos: application to chaotic encryption, *Int. J. Mod. Phys. B* 18 (17–19) (2004) 2415–2421.
- [14] Z. Li, D. Xu, A secure communication scheme using projective chaos synchronization, *Chaos Solitons Fractals* 22 (2004) 477–481.
- [15] E. N. Lorenz, Deterministic non periodic flow, *J. Atmos. Sci.* 20 (2) (1963) 130–141.

- [16] L. M. Pecora, T. L. Carroll, Driving systems with chaotic signals, *Phys. Rev. A* 44 (1991) 2374–2383.
- [17] R. Mainieri, J. Rehacek, Projective synchronization in three-dimensional chaotic systems, *Phys. Rev. Lett.* 82 (15) (1999) 3042–3045.
- [18] D. Xu, Z. Li, Controlled projective synchronization in nonparametrically-linear chaotic systems, *Int. J. Bifurcation Chaos* 12 (6) (2002) 1395–1402.
- [19] G. Alvarez, S. Li, F. Montoya, M. Romera, G. Pastor, Breaking projective chaos synchronization secure communication using filtering and generalized synchronization, *Chaos Solitons Fractals* 24 (3) (2005) 775–783.
- [20] T. Stojanovski, L. Kocarev, U. Parlitz, A simple method to reveal the parameters of the Lorenz system, *Int. J. Bifurcation Chaos* 6 (12B) (1996) 2645–2652.
- [21] K. M. Cuomo, A. V. Oppenheim, Circuit implementation of synchronized chaos with applications to communications, *Phys. Rev. Lett.* 71 (1) (1993) 65–68.
- [22] G. Alvarez, S. Li, Some Basic Cryptographic Requirements for Chaos-Based Cryptosystems, accepted in 2005, tentatively scheduled for publication in *Int. J. Bifurcation Chaos*, 16 (7) (2006), preprint available online at <http://www.hooklee.com/pub.html>.